Fermilab

TM-1059-A
1183.000

THE USE OF NON-HYDROGENOUS WEDGES FOR THERAPEUTIC NEUTRON BEAM SHAPING

Randall K. Ten Haken, Miguel Awschalom, and Ivan Rosenberg

November 1981

ABSTRACT

Field shaping wedges made of Teflon, aluminum, steel, and lead were designed for a p(66)Be(49) therapeutic neutron beam. Design considerations, expectations, and actual measured changes in dose profiles are presented.

Key words: neutrons, neutron radiation therapy, wedges, p-Be, non-hydrogenous

INTRODUCTION

Teflon[1] beam-shaping wedge filters have long been used routinely at the Fermilab Neutron Therapy Facility[2] to produce better treatment dose distributions.[3,4] These wedges are manually mounted at the patient end of the collimators and have simple triangular cross-sections.

Other neutron therapy centers have used polyethylene wedges for beam shaping.[5] Hydrogenous materials, such as polyethylene, were not considered for use at this facility due primarily to the substantial hardening effect exhibited by such materials for p-Be generated neutron beams.[6] Such hardening would effect changes in the central axis depth dose characteristics of the neutron beam, an inconvenience in patient treatment planning. Furthermore, the differential hardening of the beam across the wedge due to different thicknesses of absorber would tend to decrease the effective isodose rotation angle.

Teflon offers some advantages over polyethylene: (a) due to greater density, it provides more compact wedges, and (b) it absorbs the proton recoils from the internal surfaces of the hydrogenous collimators[7], without adding a significant number of charged particles of its own.[8] Two

advantages of Teflon over metals, which also share some of the above properties, are lower remanent radioactivity and lower total weight for the same wedge effect, important features for a manual system.

In the next generation of neutron therapy units, however, the use of rotational gantries and non-hydrogenous adjustable collimators will permit the placement and storage of remotely controlled wedge filters at the target end of the collimator, a high radiation area. In that case, compactness and resistance to radiation damage will be more important than low remanent radioactivation and weight, and the use of metals may become advisable. This note investigates the possibility of using such materials for construction of wedge filters and presents criteria for their design.

Wedge Design

A simple argument for the prediction of isodose rotation by wedges with simple triangular cross-section is presented here. No attempt is made to analyze wedges based on the shape of the open isodose curves.[9] Triangular shaped wedges have predictable effects on the rotation of the tangent to the isodose curves at the central axis. To produce a

rotation of that tangent through an angle Θ (see Fig. 1) the angle α of the wedge must be such that the extra beam attenuation due to the thickness $\underline{a}$ of wedge material compensates for the attenuation that would have occured in the corresponding phantom thickness $\underline{A}$. In the limit of small angles Φ, close to the central axis, this requirement reduces to the following relationship:

$$\frac{\tan \alpha}{\lambda} = \frac{R}{r} \frac{\tan \theta}{\lambda_{eff}} = \frac{SSD+z}{SWD} \frac{\tan \theta}{\lambda_{eff}} , \qquad (1)$$

where λ is the initial narrow beam kerma attenuation length in the wedge material for the given neutron beam;[10] λ_{eff} is the effective attenuation length of the neutron beam in the phantom, calculated from the slope of central axis depth dose curve at the depth z in question; and SSD (the Source-Skin Distance), SWD (Source-Wedge Distance), $\underline{R}$ and $\underline{r}$ are defined in Fig. 1.

A few consequences of this relationship are worth discussing. At the depth of maximum dose (100% isodose) λ_{eff} becomes infinite. Equation 1 leads to the requirement that the tangent to the 100% isodose at the central axis should be rotated through 90°, i.e. parallel to the central axis, for all wedge angles. This is, in fact, observed.[13] For a given wedge, the angles through which the isodoses are rotated

depend on several factors, such as SSD, depth in tissue, and field size. In isocentric treatments the effective rotation of the reference isodose is altered as the SSD is varied, being larger for shorter SSD's. When different isodose levels are considered, the rotation angle becomes steadily smaller as the depth is increased, due to the same geometrical effect. As the value of λ_{eff} depends on field size, the effect of the wedge filter will change with field size, even when all other factors are kept constant. Furthermore, if the wedge material has a hardening effect on the beam,[6] the shape of the rotated isodoses away from the central axis cannot be predicted simply from the unwedged isodoses and the wedge attenuation profile,[9] owing to the differential hardening of the beam by varying thicknesses of the wedge. Considering these factors, the properties of neutron wedge filters should be specified with care.

Of course, these influences have been known and discussed for a long time,[11] especially in relation to lower energy x-ray beams. However, they have been rather overlooked in wedge design and specification for megavoltage beams where they are less important. Neutron beams, though, even if they can approach megavoltage X-ray beams in penetration[12], have scatter properties closer to those of lower energy photon beams, and thus the factors mentioned above must be kept in mind.

It also follows from the above expression that, if the same rotation of isodose curves is required using wedges made out of different materials, the angles of the wedges must satisfy the following relationship:

$$\frac{\tan \alpha}{\lambda} = \text{constant} \qquad (2)$$

for the same relative geometry and neglecting any differences in beam hardening.

Attenuation Length Measurements.

A beam with a nominal field size of 8x8 cm^2 at an SAD of 190 cm [13] was used for "narrow beam" attenuation measurements.[10,14] Samples were placed at the end of the collimator (109 cm from the neutron source) and a detector was placed at 190 cm from the source. The detector consisted of a 1 cm^3, air filled, A-150 TE-plastic ionization chamber having 5 mm thick walls and covered with a 9 mm thick build-up cap made of the same material. For each material under investigation (Teflon, aluminum, lead and steel) the kerma transmission of the p(66)Be(49) neutron beam was measured for several absorber thicknesses.

When investigated over a large attenuation range, neutron beam attenuation curves may not be described well by a simple exponential.[10,14] However, an exponential is a satisfactory approximation over the small attenuation ranges relevant to this work. The values of kerma attenuation length (λ) shown in Table 1 were, therefore, obtained by a least square fit of the expression $I_t = I_o\, e^{-t/\lambda}$ to the kerma transmission data.

Wedge Effect Measurements.

Using the attenuation lengths computed from the measurements described above, together with the relation in Equation 2, wedges were designed and constructed out of aluminum, lead and steel to produce the same effect as the Teflon wedges now in use[13]. The corresponding physical wedge angles are given in Table 1. The test wedges were manufactured to just cover the downstream collimator apertures for the two field sizes used in this study. Thus, the thin edge of each wedge was always at the field edge. The transmission through the thick edge of each wedge is shown in Table 1. The effect of these wedges was measured in a TE-liquid phantom[15] using the same thimble chamber, electronics, and geometry as for the earlier measurements.[13]

The modified off-axis ratios were measured for each shallower angle metal wedge at two depths, 2 cm and 10 cm, for a nominal 10x10 cm^2 collimator,[13] at an SSD of 180 cm. For steel and aluminum, measurements were also made with steeper angle wedges at depths of 2 cm and 20 cm for a nominal 20x20 cm^2 collimator. The latter measurements provide a more stringent test of the design criteria, even though they are of less clinical significance.

Results and Discussion.

Application of Eq. 1 using the information contained in Table 1 and values of λ_{eff} deduced from central axis depth dose data[13] leads to predictions that can be checked against the measured isodose rotation angles.[13] The predicted rotation of the tangent to the 90% isodose at the central axis of a 10x10 cm^2 field size at 180 cm SSD is 40° using the shallower wedges. The predicted rotation for the same isodose, at 5 cm deep, with the 20x20 cm^2 field under the same conditions, but with the steeper wedges, is 59°. The rotation angles actually measured are 40° and 55°, respectively. Reasonably good agreement is thus obtained at this shallow depth. Agreement, however, is not as good at greater depths. At 10 cm deep with the 10x10 cm^2 field size, for example, the predicted and measured rotation angles using the shallower wedges are 35.5° and 33.5°, respectively. For the 20x20 cm^2 field at 20 cm deep, the corresponding values are 52° and 44.5°, using the steeper wedges. These discrepancies are probably due to the influence of scattered radiation, which was not explicitly accounted for in Eq. 1, and which becomes increasingly more important for larger field sizes and at greater depths.

Once a given wedge angle is chosen, however, wedges constructed from different materials through use of Eq. 2 produce nearly identical effects. This is shown by the profiles measured for aluminum, lead and steel which are compared to earlier Teflon measurements and to each other in Figs. 2 and 3.

As can be seen from the shallower angle wedge data in Figs. 2(a) and 2(b), the profiles modified by wedges of different materials are practically indistinguishable from one another. In fact, the off-axis ratios at the high-dose side of the various wedges agree with one another to better than $\pm$1% at both depths. For these wedges, the maximum attenuation, at the low-dose side, is about 32% (Table 1). This attenuation is expected to increase the depth for half-maximum dose, which is about 16 cm for the open beam,[6,13] by about 4 mm for steel and 7 mm for Teflon.[6] These slight differences in the hardening properties of the materials do not noticeably affect the profiles at the depth of 10 cm. Furthermore, the increase in the central axis penetration, roughly half of that expected at the low-dose side, would be hardly noticeable in routine treatment planning.

The profiles measured for the steeper angle wedges shown in Figs. 3(a) and 3(b) exibit some small differences among materials. At a depth of 2 cm, the high-dose side peaks of the off-axis ratios have a spread of $\pm$2%, while at 20 cm deep, the spread is $\pm$1.3%. These differences could be accounted for by a combination of uncertainties in attenuation measurements, wedge manufacture and material reproducibility (Table 1). The narrowing of these differences at the greater depth could be due in part to differential hardening. At the low-dose side of the wedge, where the attenuation is about 72% (Table 1), the increase in the depth of half-maximum dose is expected to be 9 mm for steel but 15 mm for Teflon[6]. Hardening, of course, is negligible at the high-dose side, where there is no attenuation. This differential hardening across the wedge would decrease the peak at the high-dose side of the profile relative to the central axis, when measured at depth, and do so more for Teflon than for steel. The overall effect, however, is seen to be small even at a depth of 20 cm. The increased penetration at the central axis, an addition of 10 mm to the depth for half-maximum dose when using the Teflon wedge, could affect central axis dose calculations. However, the combination of such a large field size and such a steep wedge is extremely rare in actual practice.

CONCLUSIONS

The rotation of isodose curves at the central axis of a neutron beam by non-hydrogenous wedges can be predicted from the narrow beam kerma transmission properties of the wedge material and the central axis depth dose characteristics of the neutron beam.

For isocentric gantries where wedges may be mounted in the gantry near the target end of the collimator, space will be at a premium, radiation damage could be significant and remanent radioactivity should not be critical. Therefore, due to its large attenuation and small hardening effect, steel appears to be a material of choice for wedge construction.

If wedges are used at the patient end of the collimator, weight, hardening, and radioactivation considerations dictate the use of Teflon, rather than polyethylene or metals, as a wedge material of choice.

Acknowledgements

We wish to thank B. Bennett and B. Pientak who helped in taking the measurements and M. Gleason who helped prepare this manuscript. This work was partly supported by NCI Grant 5PO1CA18081-06.

REFERENCES

1. Trade name of E. I. DuPont de Nemours, & Co., Inc.

2. L. Cohen, M. Awschalom, "The Cancer Therapy Facility at the Fermi National Accelerator Laboratory, Batavia, Illinois, a Preliminary Report", Applied Radiology, 5 ,51 (Nov.-Dec., 1976).

3. M. Awschalom, I. Rosenberg, "Neutron Beam Calibration and Treatment Planning", Fermilab Internal Report, TM-834, Dec. 6, 1978.

4. M. Awschalom, I. Rosenberg, R. Ten Haken, L. Cohen, F. Hendrickson, "The Fermilab Neutron Therapy Facility Treatment Planning for Neutron and Mixed Beams", Workshop on Treatment Planning for External Beam Therapy with Neutrons, Technische Universitat, Munchen, Germany, Sept. 17-19, 1980.

5. M. Catterall and D. K. Bewley, "Fast Neutrons in the Treatment of Cancer", Academic Press: London, 1979.

6. I. Rosenberg, M. Awschalom, R. K. Ten Haken, "The Effects of Hydrogenous and Non-hydrogenous Filters on the Quality of a p(66)Be(49) Neutron Beam", preceding paper.

7. L. S. August, P. Shapiro, L. A. Beach, "The Light-ion Flux Mixed With Collimated Fast-neutron Beam", Phys. Med. Biol., 25, 573.

8. M. Awschalom, I. Rosenberg, "Characterization of a p(66)Be(49) Neutron Therapy Beam. II. Skin-sparing and Dose Transition Effects", Med. Phys. 8 , 105 (1981).

9. H. E. Johns & J. R. Cunningham, The Physics of Radiology, 3rd Ed. 5th Print., Springfield, Illinois: C.C. Thomas, 1978.

10. M. Awschalom, A. Hrejsa, I. Rosenberg, R. K. Ten Haken, "Kerma Transmission for Various Materials for a p(66MeV) Be(49MeV) Neutron Beam", Health Physics, 41, 184-187, 1981.

11. W. J. Meredith & J. B. Massey, Fundamental Physics of Radiology, 3rd Ed., Chicago: Year Book Medical Publishers, 1977.

12. R. K. Ten Haken, M. Awschalom, F. Hendrickson, I. Rosenberg, "Comparison of the Physical Characteristics of a p(66)Be(49) Neutron Therapy Beam to Those of Conventional Radiotherapy Beams", to be published.

13. I. Rosenberg, M. Awschalom, "Characterization of a p(66)Be(49) Neutron Therapy Beam: I. Central Axis Depth Dose and Off-axis Ratios", Med. Phys., 8, 99 (1981).

14. F.H. Attix, R.B. Theus and G.E. Miller, "Attenuation Measurements of a Fast Neutron Radiotherapy Beam", Phys. Med. Biol. , 21 , 530 (1976).

15. N. A. Frigerio, R. F. Coley, M. J. Simpson, "Depth Dose Determination I. Tissue Equivalent Liquids for Standard Man and Muscle", Phys. Med. Biol. 17 , 792 (1972).

TABLE 1

Physical Properties of Wedges Made Our of Different Materials.

Material	Density	Initial Attenuation Length (λ)		Wedges #1 (a)		Wedges #2 (a)	
				Physical Angle (α)	Transmission at Thick End	Physical Angle (α)	Transmission at Thick End
	($g\ cm^{-3}$)	cm	$g\ cm^{-2}$				
Teflon	2.1	9.0	19	$30^{o}\ 58'$	.68	$45^{o}\ 0'$	.28
Aluminum (Mg alloy)	2.7	9.7	26	$32^{o}\ 54'$	.68	—	—
Aluminum (Cu alloy)	2.8	9.5	27	—	—	$46^{o}\ 24'$	.28
Lead	11.3	6.5	73	$23^{o}\ 19'$	.68	—	—
Steel	7.9	4.6	36	$16^{o}\ 52'$	.68	$26^{o}\ 50'$	.28
Notes		(b)		(c)	(d)	(c)	(e)

Notes:
(a) Wedges No. 1 rotate the 90% isodose of the p(66)Be(49) neutron beam through 40^{o} at the central-axis. This isodose is at a depth of 5 cm for a 10x10 cm^2 field size at SSD = 180 cm. Wedges No. 2 rotate this isodose through 55^{o} for a 20x20 cm^2 field under the same conditions.
(b) As defined by $I_t = I_o\ e^{-t/\lambda}$ initial attenuation curve.
(c) As defined by $(\tan \alpha/\lambda)$ = constant.
(d) At the edge of a 10 cm wide field.
(e) At the edge of a 20 cm wide field.

Figure Captions

Fig. 1. Geometrical relationship between source, wedge, phantom, and tangent to isodose curve at central axis, defining terms used in the text.
Distances R and r , measured from the central axis,
are defined by an arbitrary ray from the source
at an angle Φ from the central axis.
Distances A and a are measured along this ray.

Fig. 2. Off-axis ratios for shallower angle wedges made out of:
Teflon (●), Aluminum (Δ), Lead (□), and Steel (o).
10x10 cm^2 collimator at an SSD of 180 cm.
All measurements are normalized to unity at the central axis.
(a) 2 cm deep in TE solution.
(b) 10 cm deep in TE solution.

Fig. 3. Off-axis ratios for steeper angle wedges made out of:
Teflon (●), Aluminum (Δ), and Steel (O).
20x20 cm^2 collimator at an SSD of 180 cm.
All measurements are normalized to unity at the central axis.
(a) 2 cm deep in TE solution.
(b) 20 cm deep in TE solution.

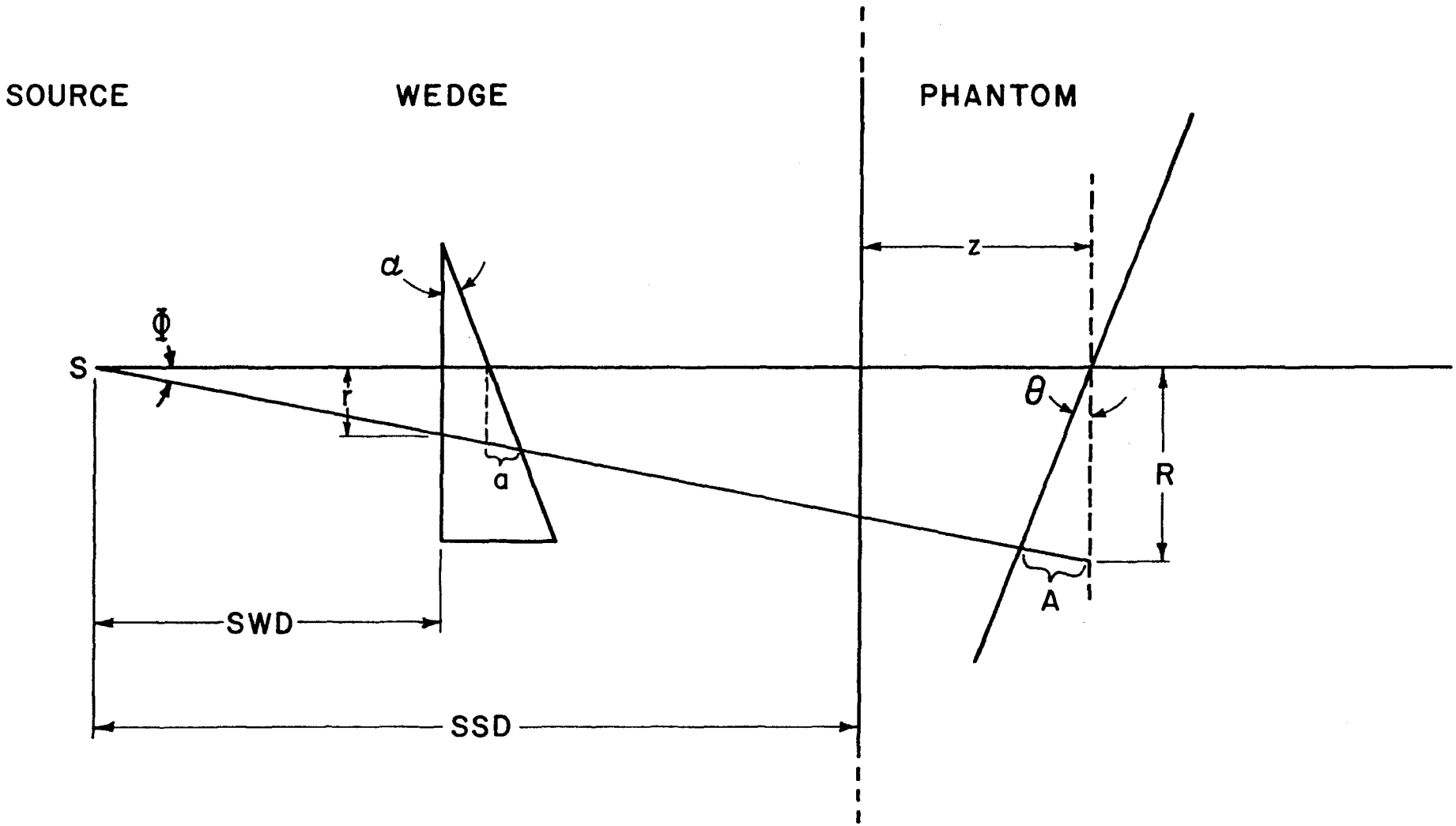

Fig. 1

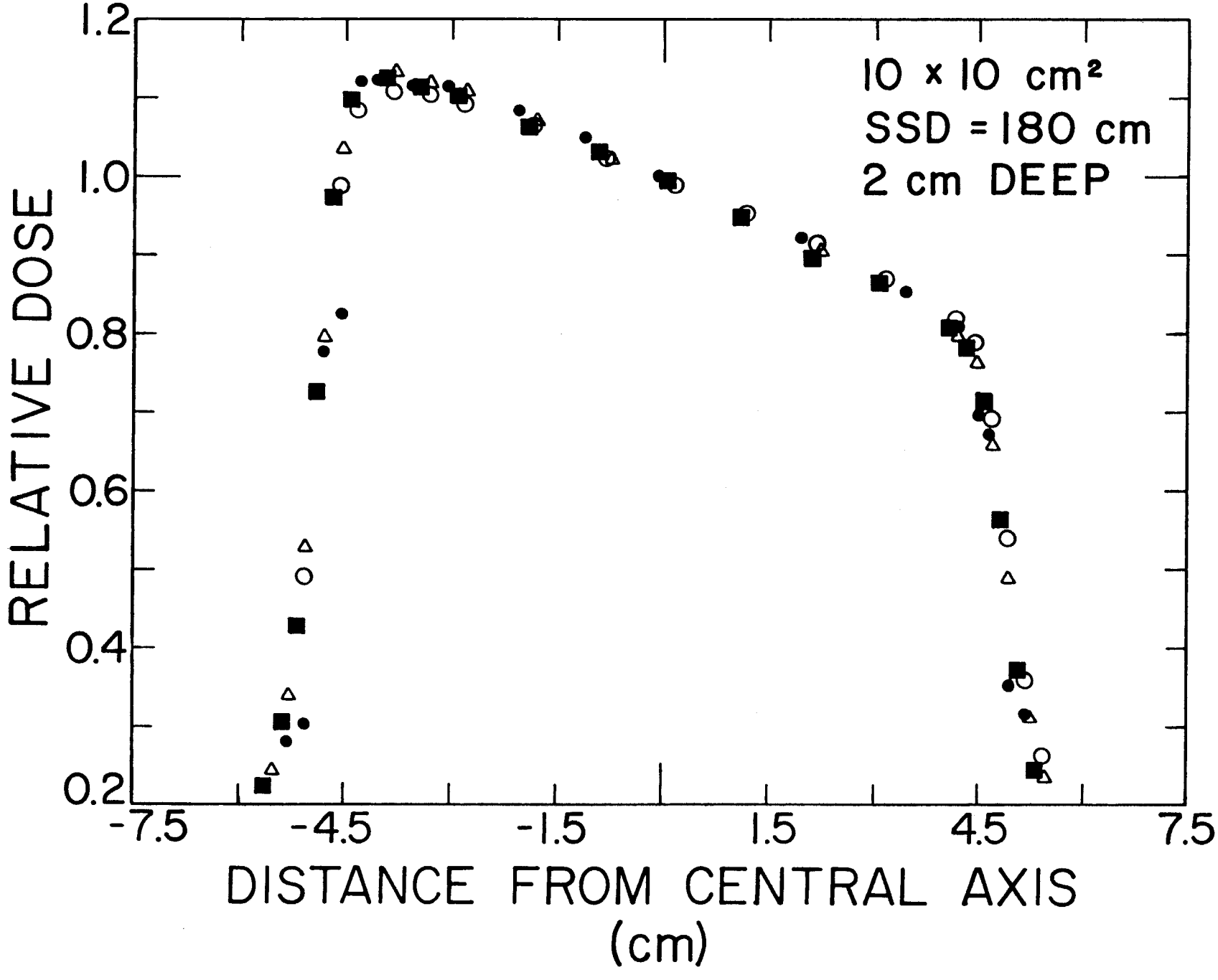
10 x 10 cm²
SSD = 180 cm
2 cm DEEP
RELATIVE DOSE
1.2
1.0
0.8
0.6
0.4
0.2
-7.5
-4.5
-1.5
1.5
4.5
7.5
DISTANCE FROM CENTRAL AXIS
(cm)

Fig. 2a

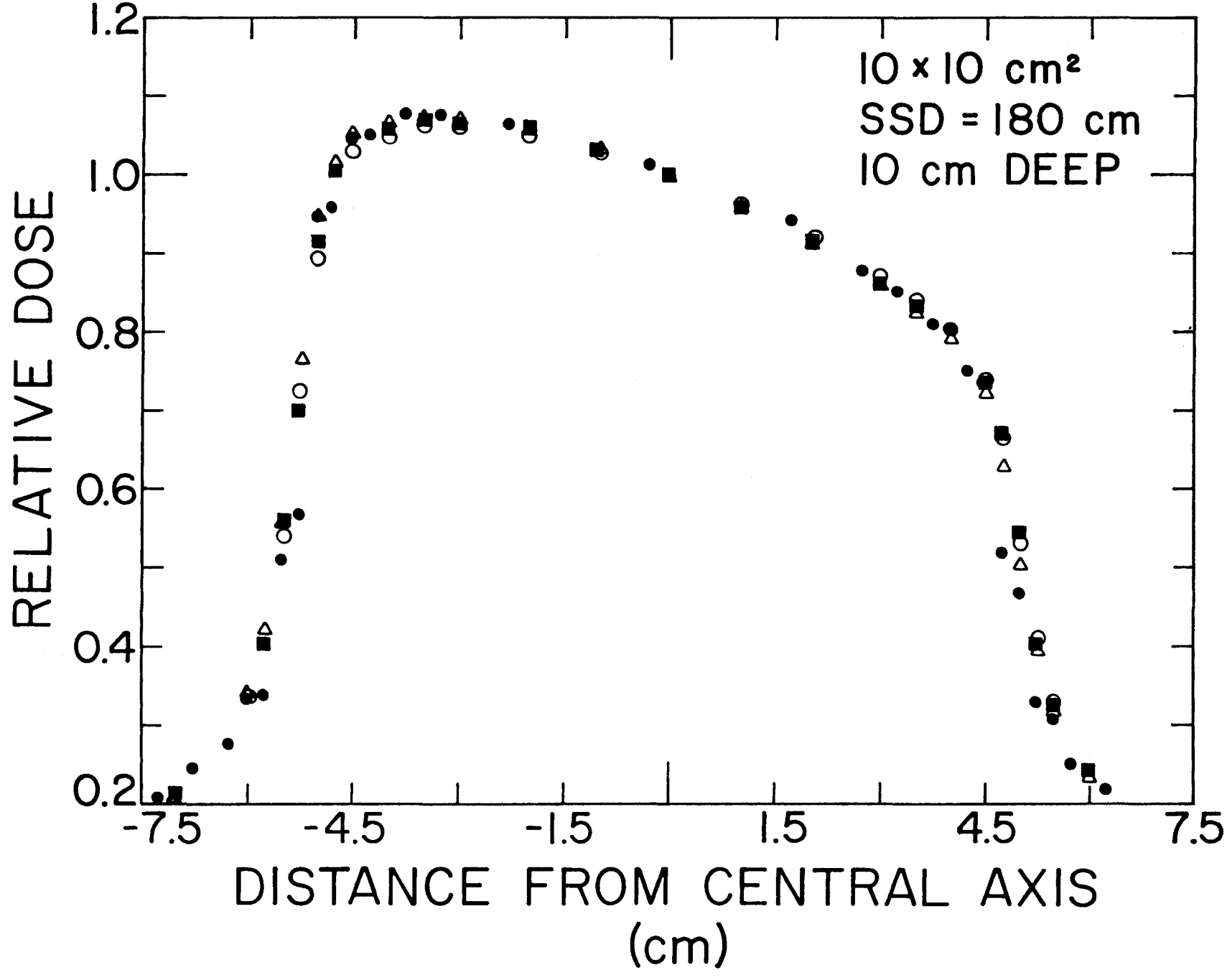
10 x 10 cm²
SSD = 180 cm
10 cm DEEP
RELATIVE DOSE
1.2
1.0
0.8
0.6
0.4
0.2
-7.5
-4.5
-1.5
1.5
4.5
7.5
DISTANCE FROM CENTRAL AXIS
(cm)

Fig. 2b

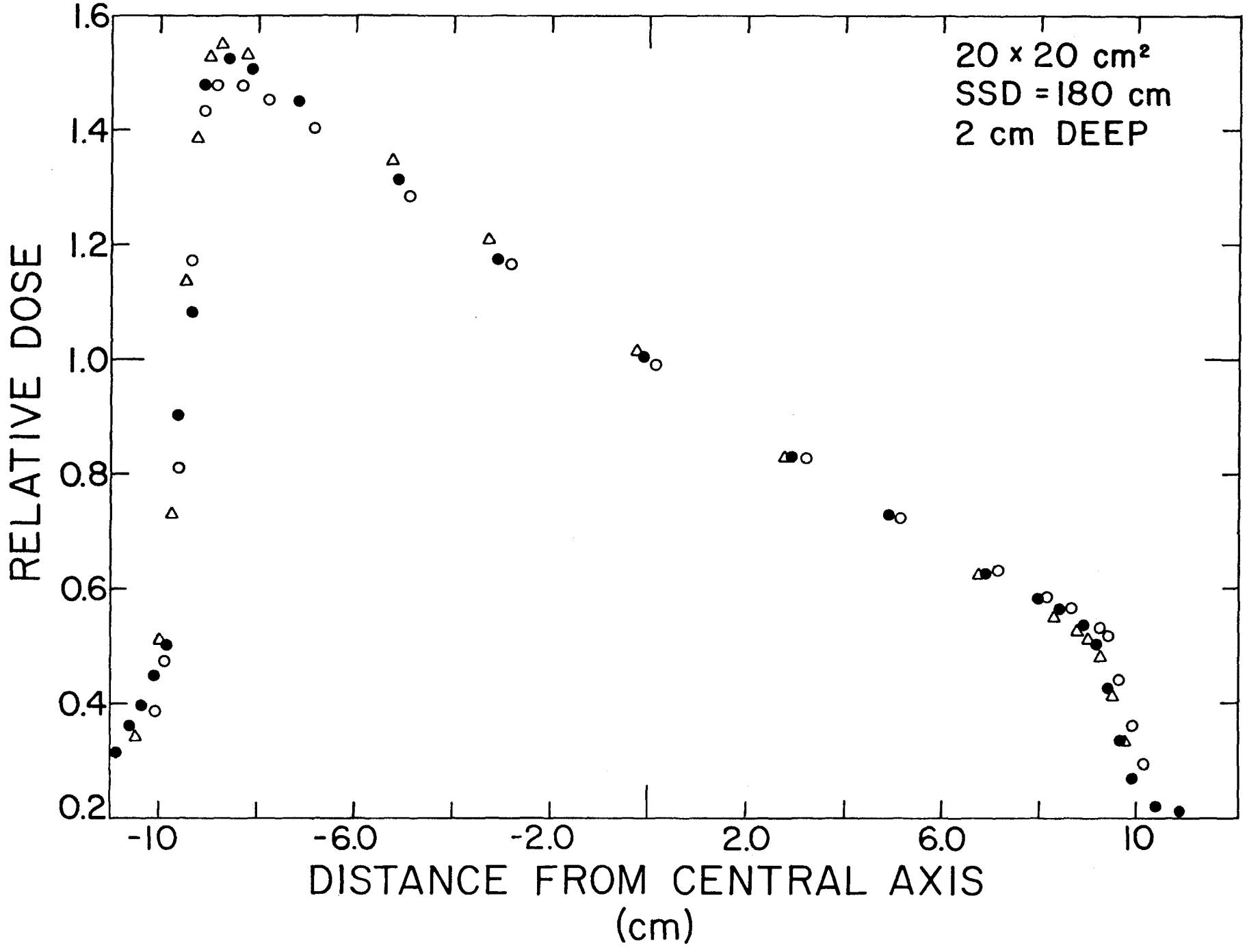
20 x 20 cm²
SSD = 180 cm
2 cm DEEP
RELATIVE DOSE
1.6
1.4
1.2
1.0
0.8
0.6
0.4
0.2
-10
-6.0
-2.0
2.0
6.0
10
DISTANCE FROM CENTRAL AXIS
(cm)

Fig. 3a

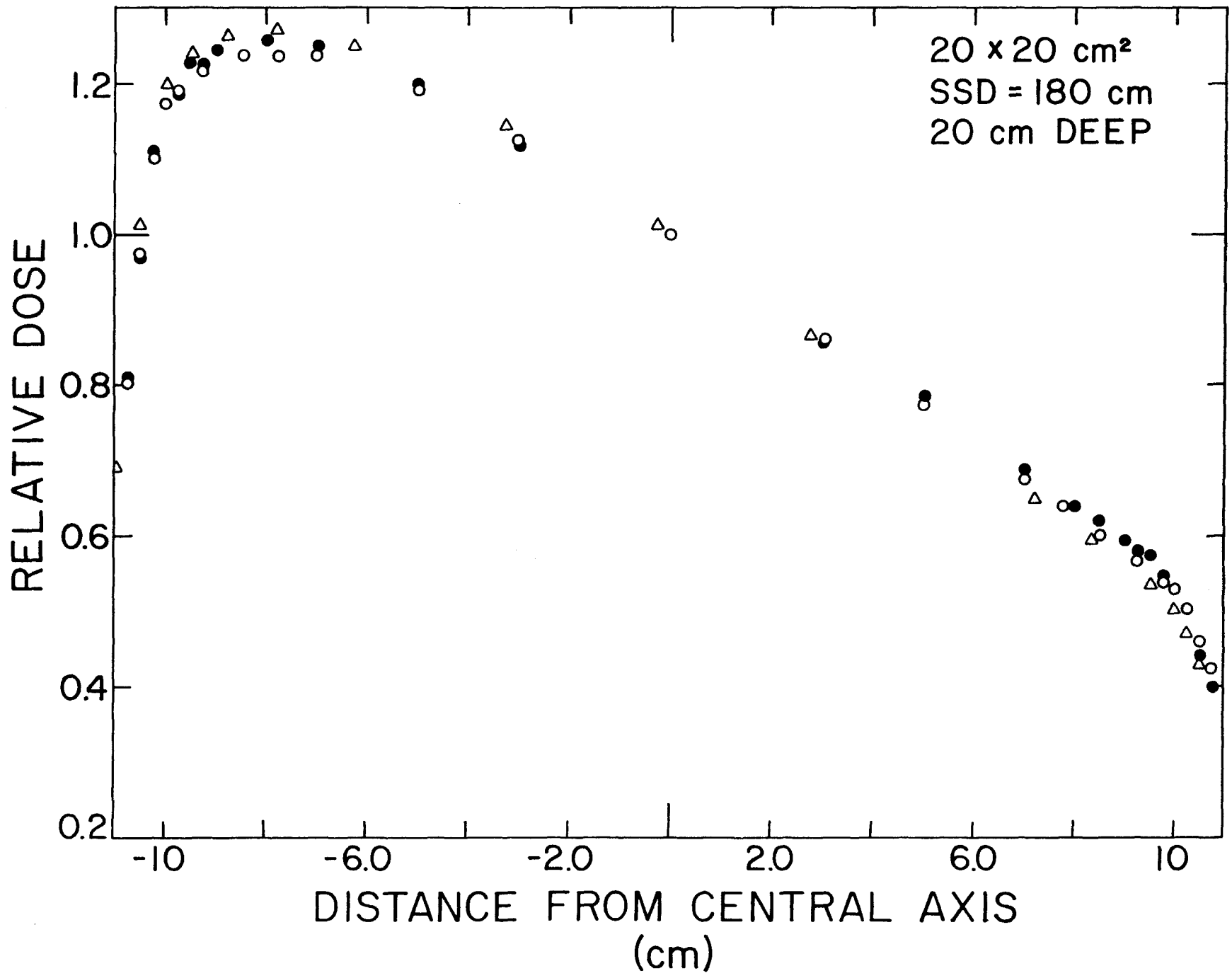
20 x 20 cm²
SSD = 180 cm
20 cm DEEP
RELATIVE DOSE
1.2
1.0
0.8
0.6
0.4
0.2
-10
-6.0
-2.0
2.0
6.0
10
DISTANCE FROM CENTRAL AXIS
(cm)

Fig. 3b